The specificity determinants for auto-proteolysis of LexA, a key regulator of bacterial SOS mutagenesis

Supporting Information

Figure S1. Sequence alignment of $LexA_{Pa}$ to similar enzymes

Figure S2. Structural homology model of the $LexA_{Pa.}$CTD

Figure S3. *In vitro* self-cleavage of purified $LexA_{Pa}$

Figure S4. Schematic of cassette mutagenesis

Figure S5. RecA*-mediated cleavage of $LexA_{Pa}$ variants from saturation mutagenesis

Figure S6. Alkali-mediated and RecA*-mediated cleavage screen of positional scanning mutants of LexA's cleavage region

Figure S7. First-order kinetic plots of cleavable $LexA_{Pa}$ point mutants from position 86 to 92

Figure S8. Mass spectrometry analysis of $LexA_{Pa}$ A89C/I94C double mutant

Figure S1. Sequence alignment of $LexA_{Pa}$ to similar enzymes. (A) Alignment of $LexA_{Pa}$ with LexA of *E. coli* and other bacterial species. Amino acid sequences of LexA of different species were obtained from Uniprot and aligned in BLAST. The full aligment between $LexA_{Pa}$ and $LexA_{Ec}$ is shown below (identity 64%). The residues surrounding LexA's scissile bond show a strong degree of conservation across species. The catalytic serine and lysine dyad are highlighted in yellow. Residues of the S1 pocked are marked by diamonds and the S3 pocket with a * demonstrating conservation of these pockets between $LexA_{Pa}$ and $LexA_{Ec}$. (B) Alignment of the cleavage region of $LexA_{Pa}$ to the cleavage region of other LexA/signal peptidase superfamily members is shown.

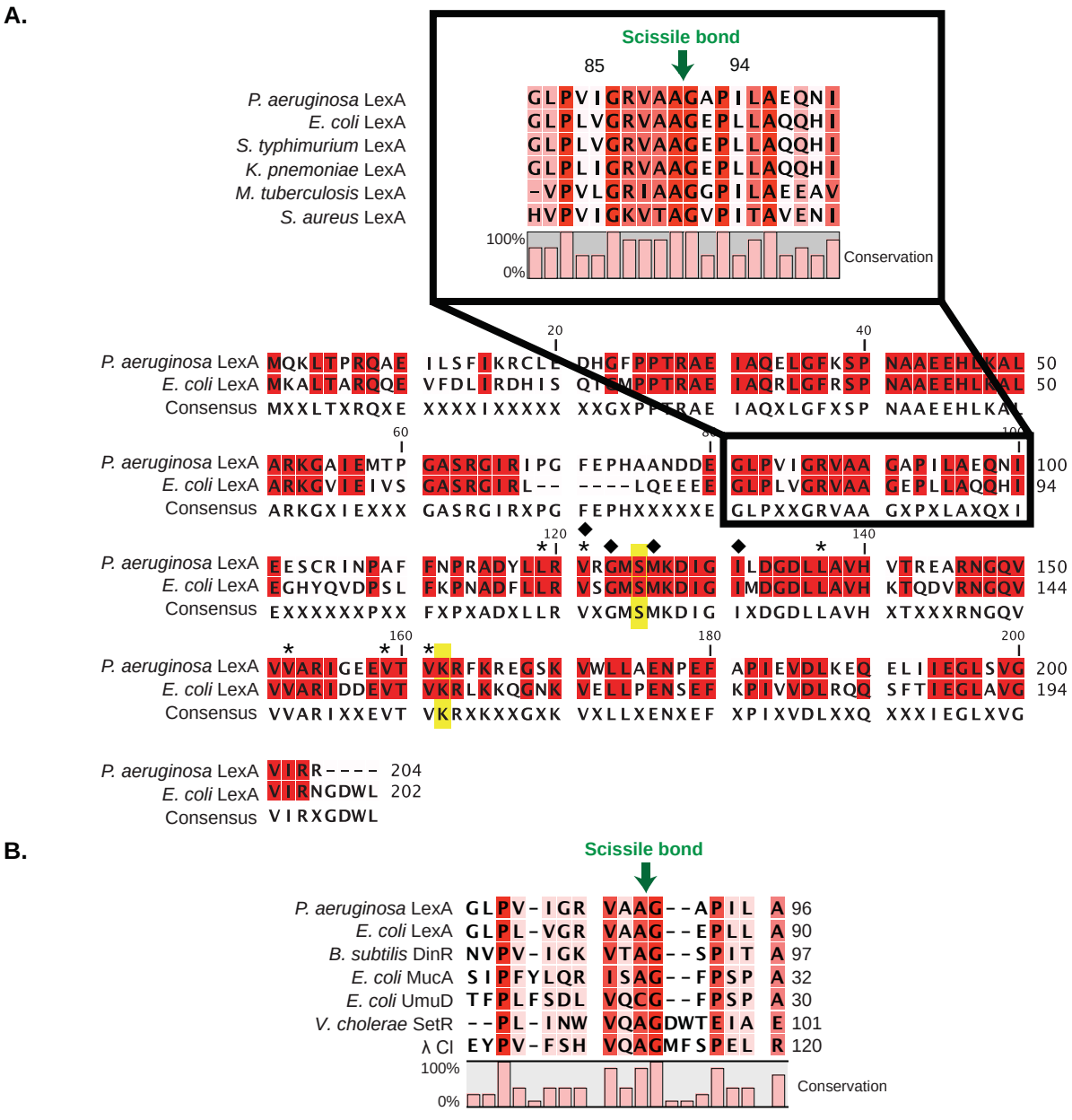
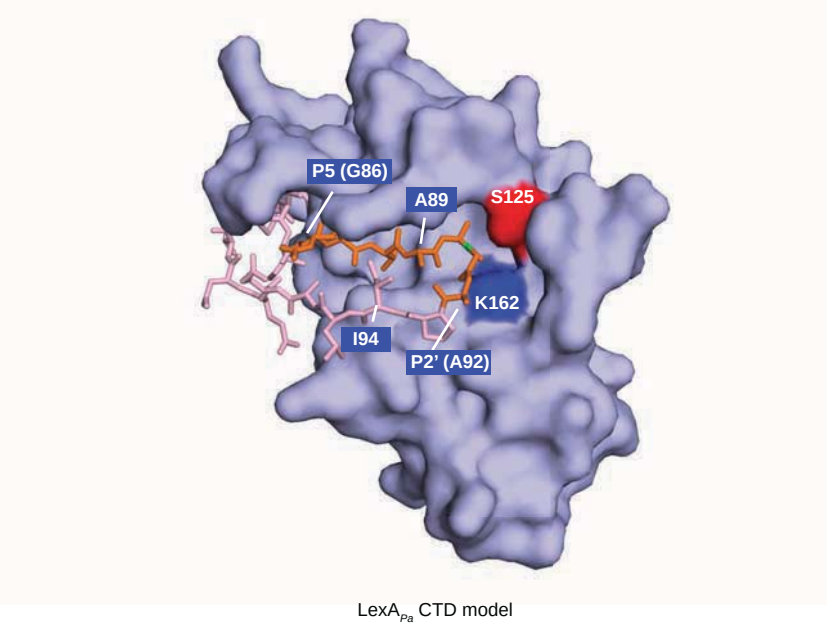


Figure S2. Structural homology model of the $LexA_{Pa.}$CTD. The model was generated with Modeller 2.0, using the active form of the *E. coli* LexA CTD as a template (PDB 1JHE). The internal peptide containing the cleavage region is shown as pink sticks, with the scissile bond between A90 and G91 colored green. The catalytic serine (S125) and basic lysine (K162) are shown as red and blue surfaces, respectively. The rest of the protein is shown as blue surface. This same model is used in Figure 6.



$LexA_{Pa}$ CTD model

Figure S3. *In vitro* self-cleavage of purified $LexA_{Pa}$. Purified wild type (WT) LexA from *P. aeruginosa* or the active site mutant S125A were incubated overnight at (A) various pH ranging from 7.2 to 11.6 or (B) in the presence or absence of RecA*. The top band (~25.7 kDa) represents full-length LexA, while two smaller bands represent the CTD (~13.8 kDa) and NTD (~11.9 kDa) after auto-proteolysis. Loss of the catalytic serine (S125A mutation) prevents auto-proteolysis under both alkali-mediated and RecA* stimulation.

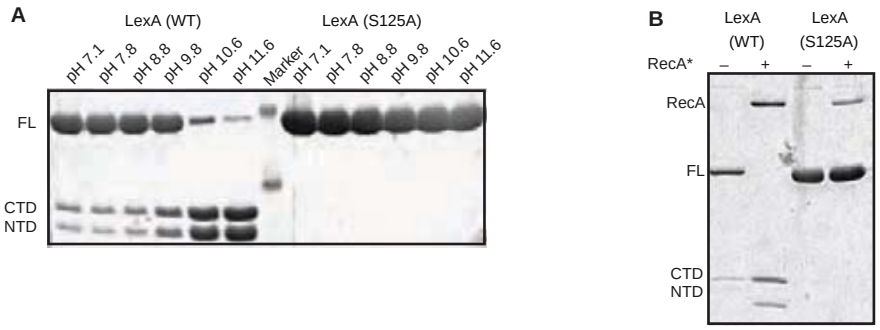


Figure S4. Schematic of cassette mutagenesis. (A) To facilitate cassette mutagenesis, mutation encoding for AgeI and EagI were introduced into positions flanking the $LexA_{Pa}$ cleavage region (red mutations). An additional internal BamHI site and a stop codon were introduced (green mutations) to facilitate high-efficiency cassette mutagenesis and to prevent the expression of the full-length LexA cloning vector gene product. (B) For cassette mutagenesis, the parent vector was digested with AgeI, BamHI and EagI. Duplexed oligonucleotide cassettes (shown in blue) containing either generate NNS codons for saturation mutagenesis or point mutations for positional scanning mutagenesis are phosphorylated and ligated into the digested vector. Note that, in addition to introducing the desired mutations, the cassette oligonucleotides revert position 95 back to a wild type leucine codon, with associated loss of the EagI site. The ligated vector was transformed into a cloning strain and the sequence confirmed. The plasmid or plasmid library (for saturation mutagenesis experiments) were transformed into BL21(DE3)-pLysS cells for expression and subsequent purification.

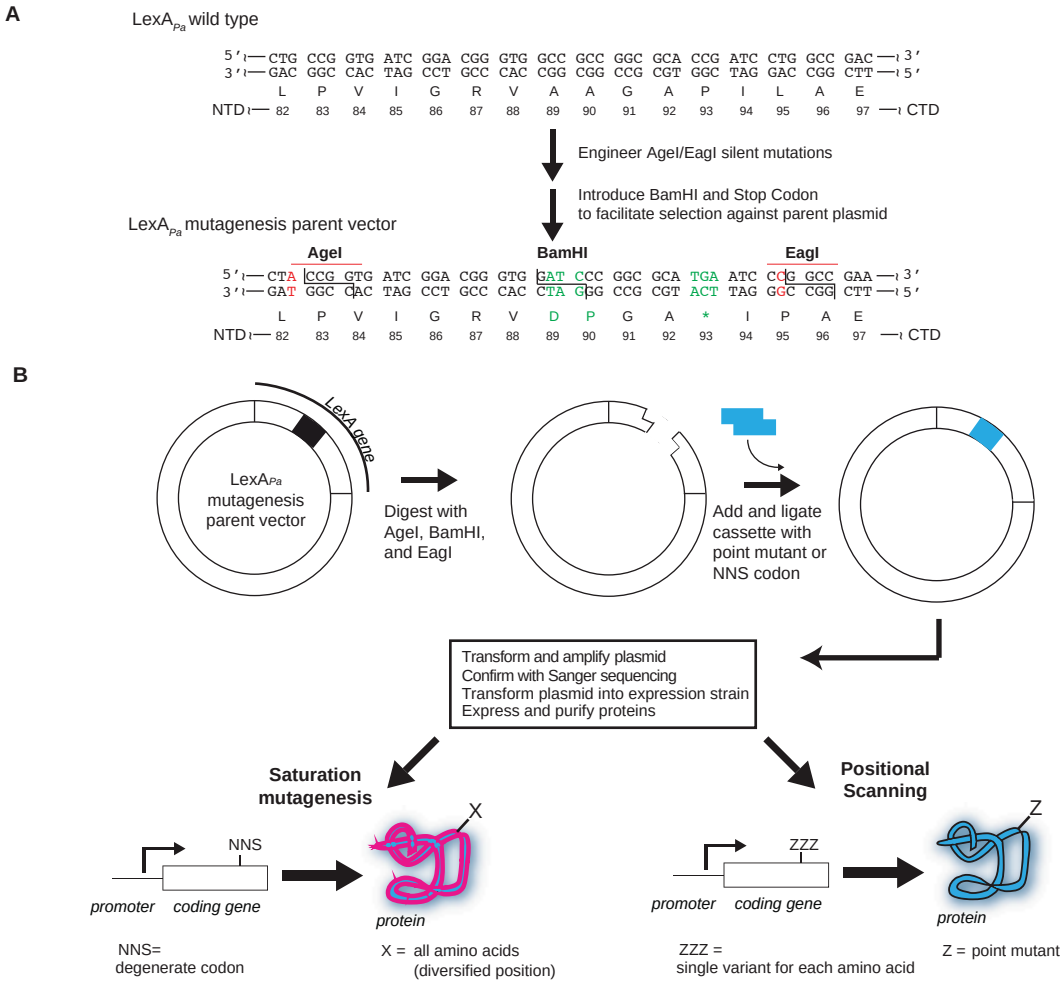


Figure S5. RecA*-mediated cleavage of $LexA_{Pa}$ variants from saturation mutagenesis. As with base-mediated cleavage, each variant, containing a single diversified position, was purified as a cohort in parallel with the wild type enzyme and subjected to overnight self-cleavage with (+) or without (-) RecA*. The fraction of cleavage product detected under each condition is shown (no RecA*, gray columns; with RecA*, black columns). Reactions were performed in duplicate and error bars reflect the standard error.

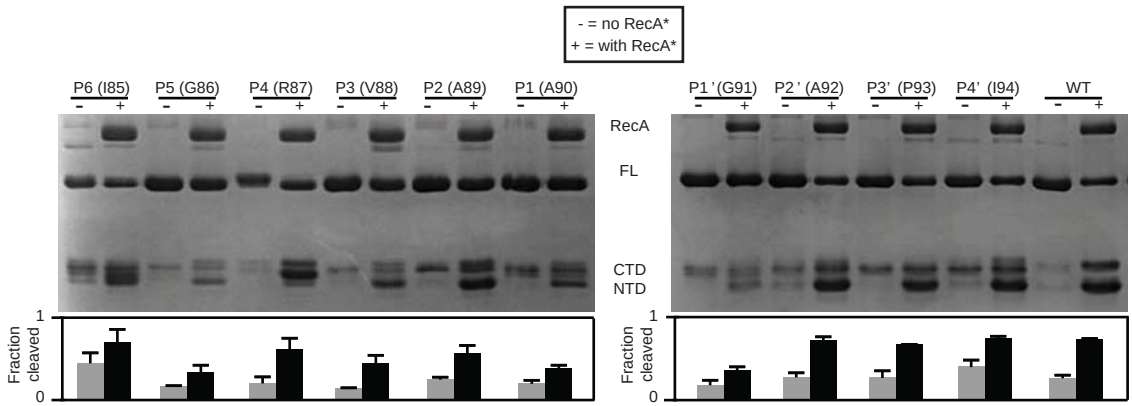
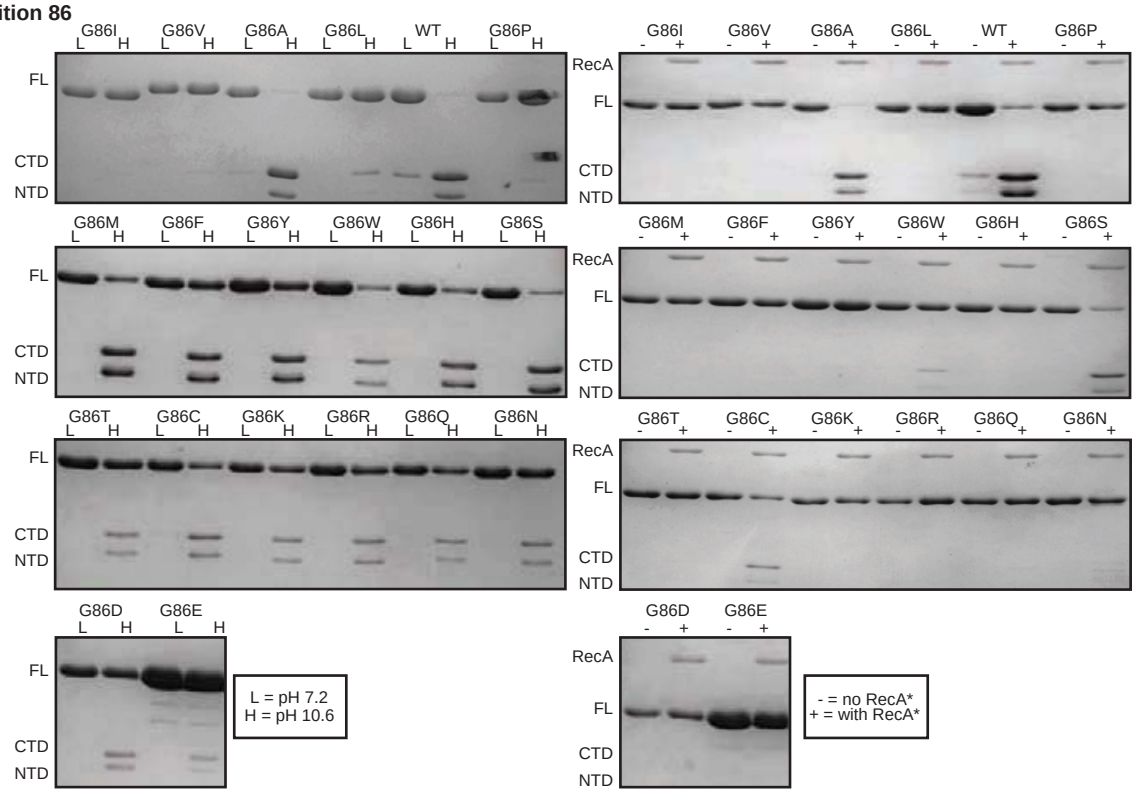
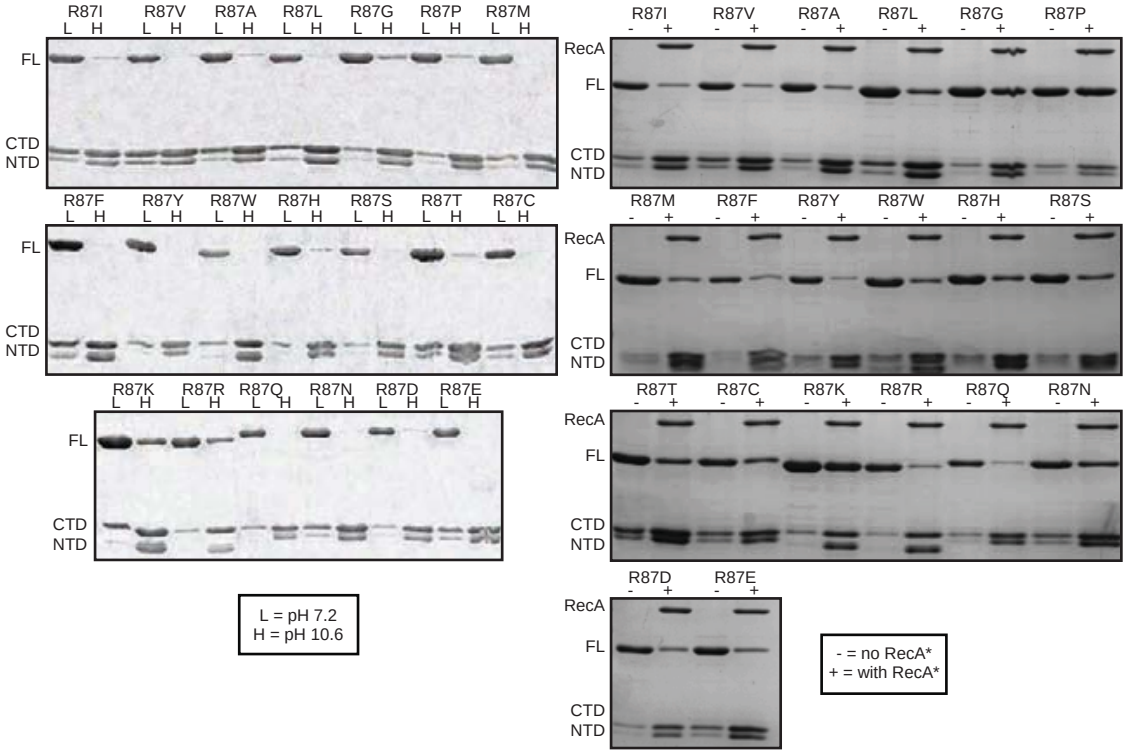


Figure S6. Alkali-mediated and RecA-mediated cleavage screen of positional scanning mutants of LexA's cleavage region. Proteins were purified in parallel at each position and subjected to two cleavage conditions. Shown are representative cleavage experiments with mutants from (A) position 86, (B) position 87, (C) position 88, (D) position 89, (E) position 90, (F) position 91 and (G) position 92. Alkali-mediated cleavage (left panels) and RecA* stimulation (right panels) produced similar cleavage profiles for all positions, with the notable exception is G86, where select mutants display basal cleavage under alkali stimulation, but not under RecA* stimulation. The alkali-mediated cleavage results for R87 and A90 are identical to those shown in Figure 4 and are included again to facilitate comparison across positions. The wild type enzyme in each batch is denoted as WT.

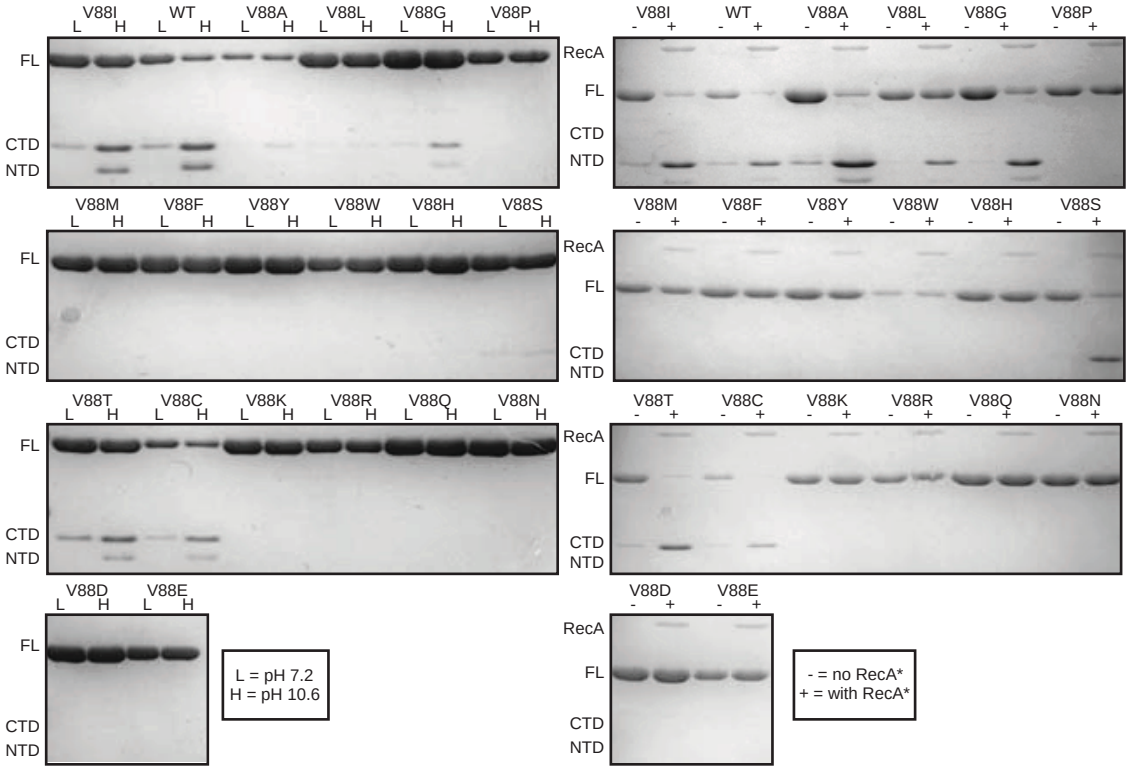
A Position 86



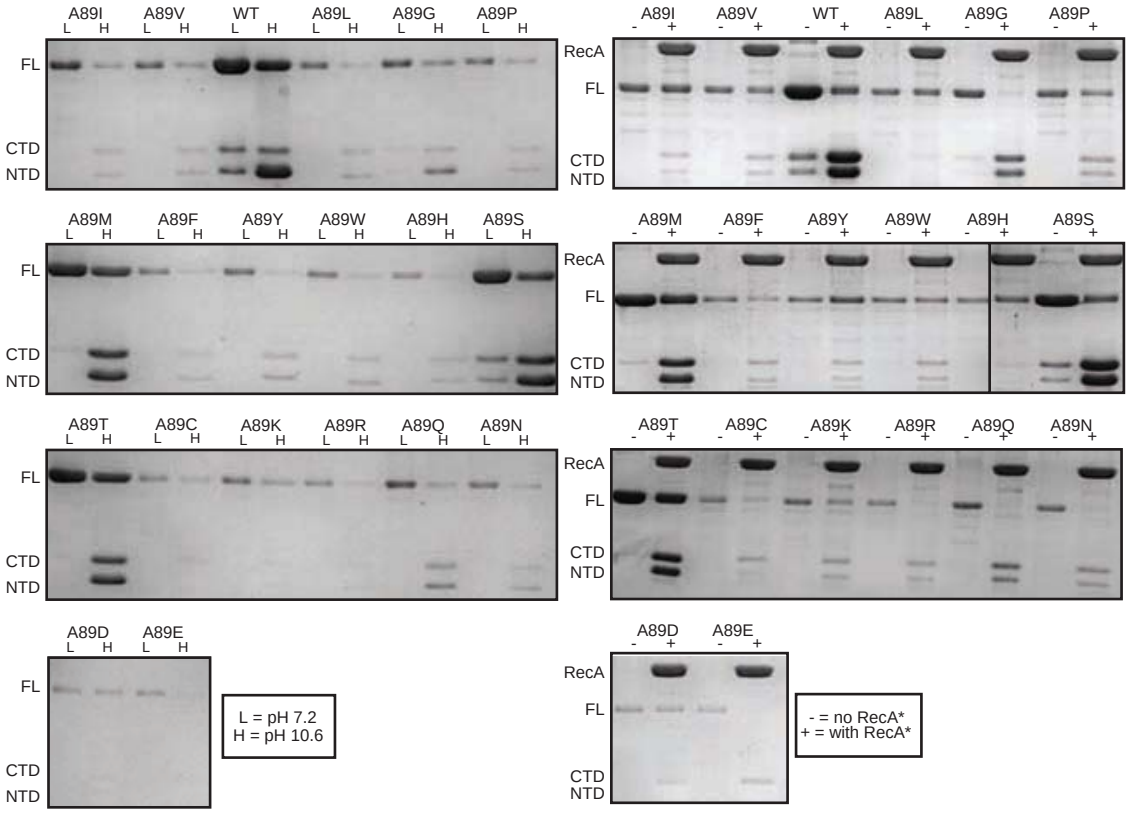
B Position 87



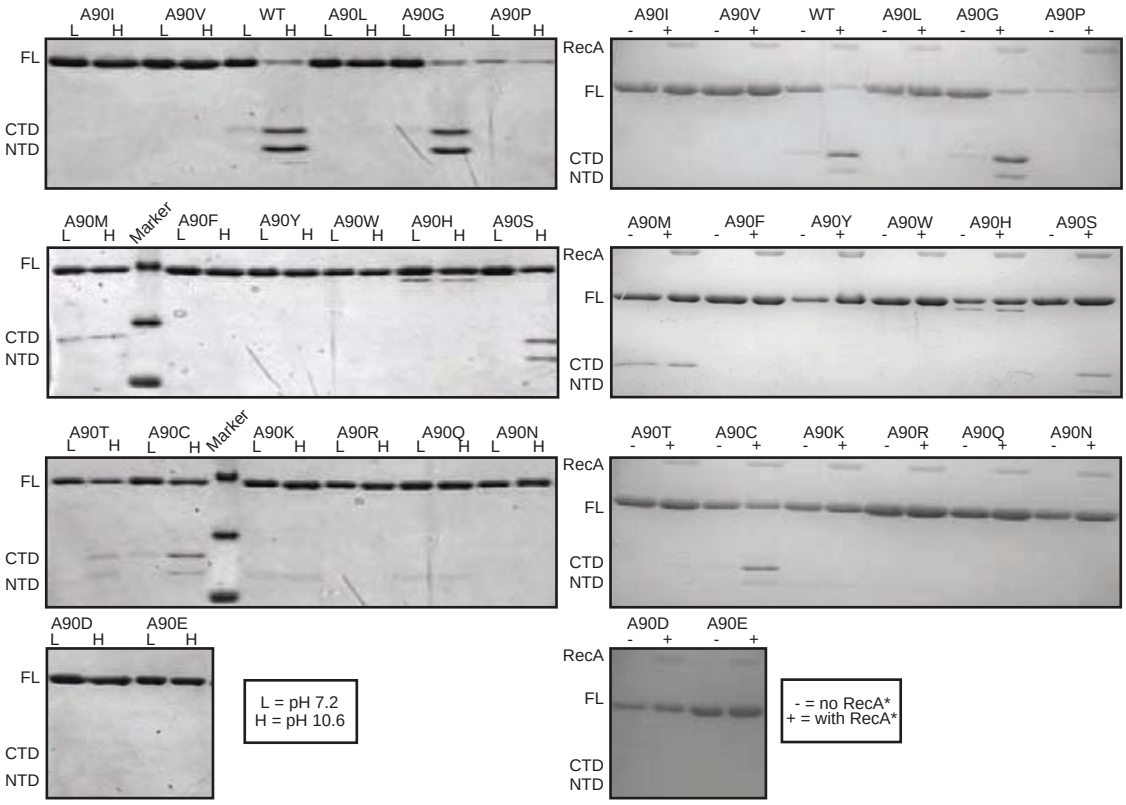
C Position 88



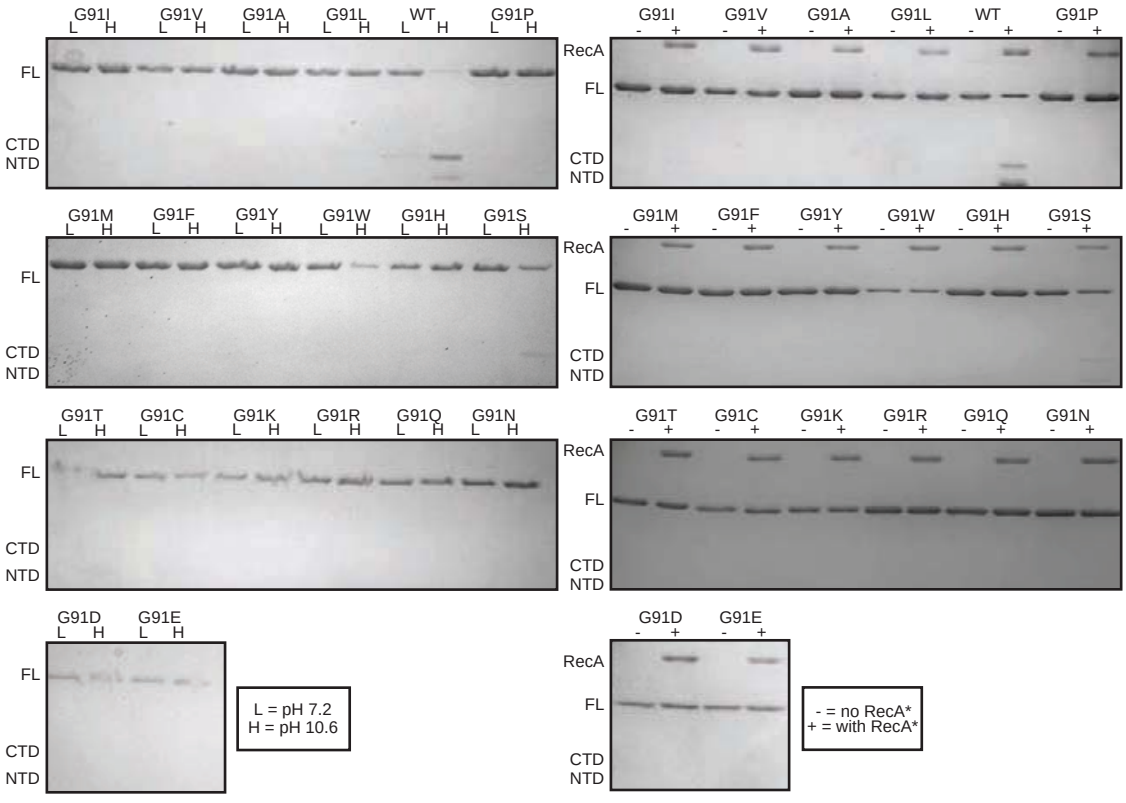
D Position 89



E **Position 90**



F **Position 91**



G Position 92

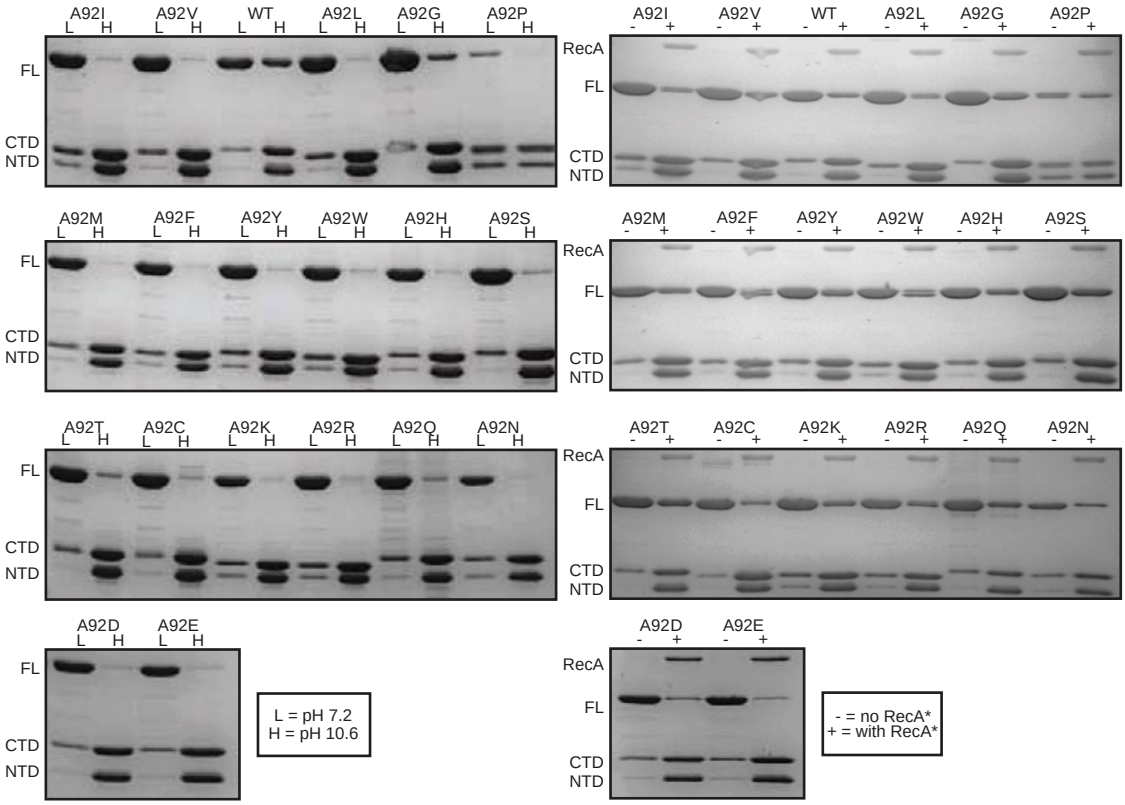


Figure S7. First-order kinetic plots of cleavable LexA$_{Pa}$ point mutants from position 86 to 92. For each plot, the bolded dashed line represents the wild type enzyme. Plots for positions 87 and 90 are identical to those in Figure 2. Mutants are grouped by the property of their side chains at physiological pH (orange: hydrophobic; purple: aromatic; yellow: hydrophilic; green: positive charge; blue: negative charge). The rates of cleavage determined by each fit are given in Table 1.

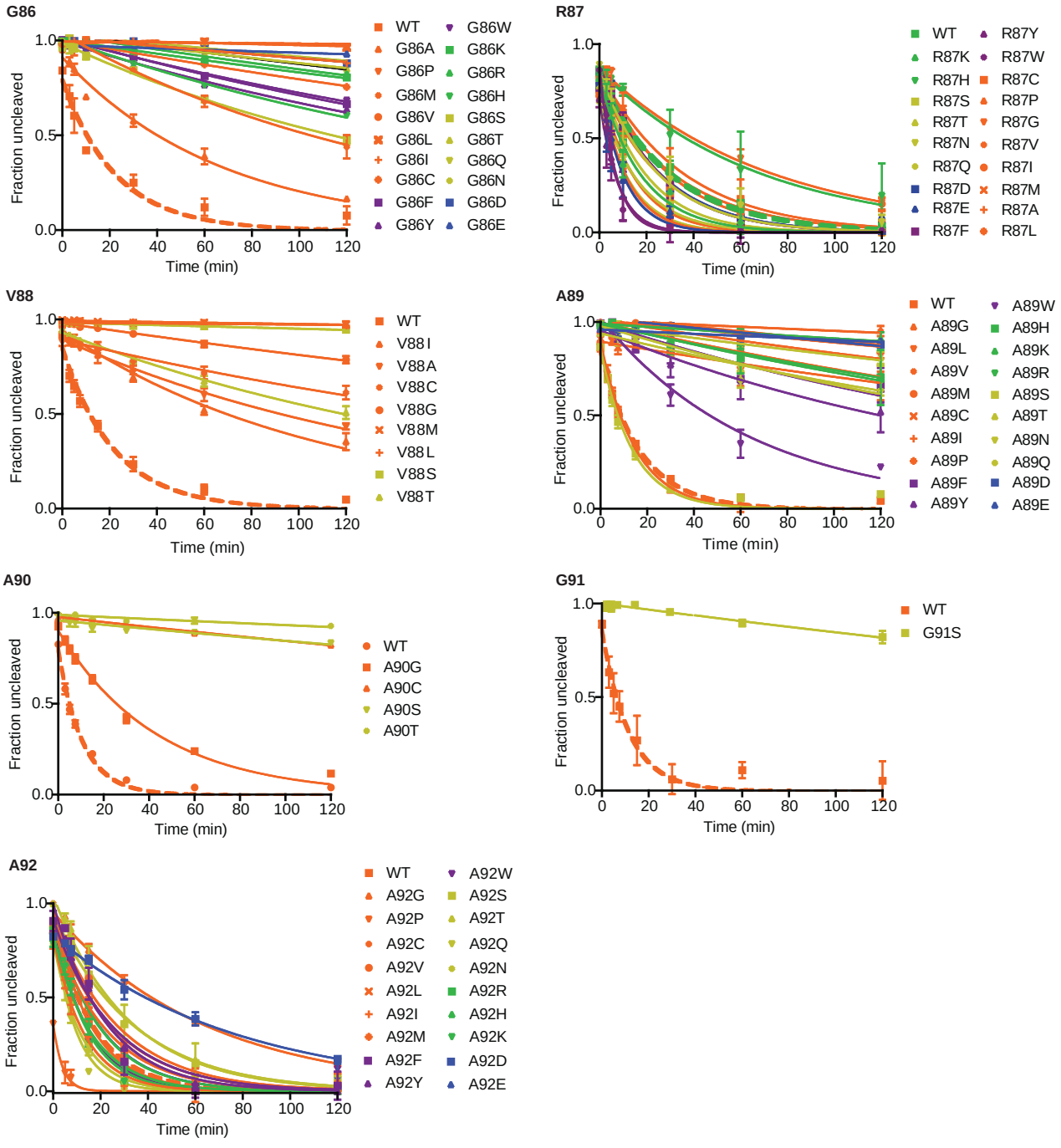
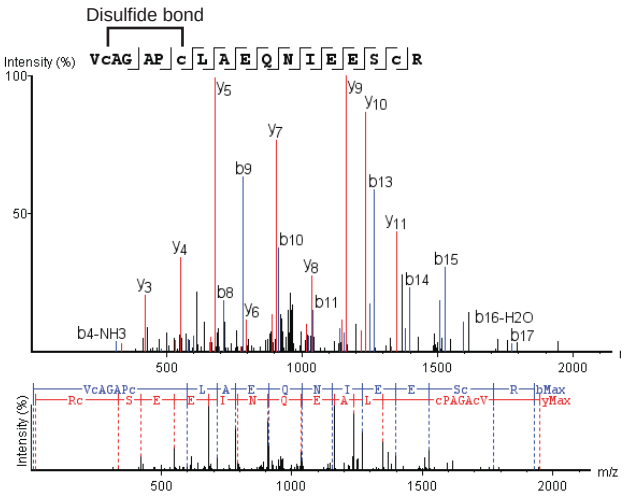


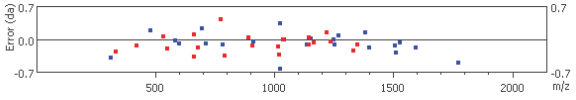
Figure S8. Mass spectrometry analysis of LexA$_{Pa}$ A89C/I94C double mutant reveals the presence of disulfides between positions 89 and 94. In the non-reduced form, residues C89 and C94 show a mass decrease of 1.01 amu, indicative of the loss of the proton of the thiol. When reducing agent is added, both residues become alkylated by the iodoacetamide. Both samples display strong -10log(P) values and the two conditions together confirm the presence of the disulfide bond.

Not reduced

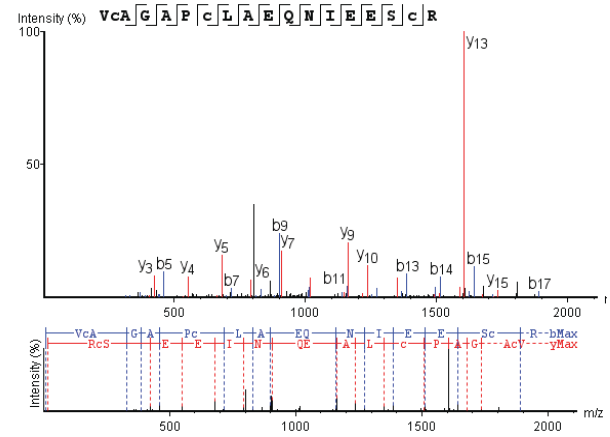


#	b	b-H2O	b-NH3	b (2+)	Seq	y	y-H2O	y-NH3	y (2+)	#
1	100.08	82.07	83.05	50.54	V					18
2	202.08	184.07	185.05	101.54	C(-1.01)	1848.77	1830.76	1831.74	924.88	17
3	273.11	255.10	256.09	137.06	A	1746.77	1728.76	1729.74	873.88	16
4	330.14	312.13	313.50	165.57	G	1675.73	1657.72	1658.70	838.36	15
5	401.17	383.16	384.15	201.09	A	1618.71	1600.70	1601.68	809.85	14
6	498.23	480.22	480.98	249.61	P	1547.67	1529.66	1530.64	774.34	13
7	600.32	582.24	583.20	300.61	C(-1.01)	1450.62	1432.61	1433.59	725.81	12
8	713.41	695.05	696.28	357.16	L	1348.74	1330.61	1331.84	674.81	11
9	784.46	766.34	767.32	392.67	A	1235.59	1217.52	1218.34	618.27	10
10	913.44	895.38	896.36	457.20	E	1164.58	1146.60	1147.42	582.75	9
11	1041.46	1024.07	1024.07	521.22	Q	1035.44	1017.60	1018.75	518.23	8
12	1155.46	1137.48	1138.57	578.25	N	907.53	889.38	890.32	454.20	7
13	1268.48	1250.57	1251.66	634.79	I	793.71	774.90	776.32	397.18	6
14	1397.79	1379.61	1380.43	699.31	E	680.46	662.14	663.62	340.63	5
15	1526.73	1508.78	1509.92	763.83	E	551.43	533.15	534.20	276.11	4
16	1613.69	1595.87	1596.67	807.35	S	422.33	404.17	405.15	211.59	3
17	1774.22	1755.71	1756.70	887.36	C(+57.02)	335.42	317.14	318.12	168.07	2
18					R	175.12	157.11	158.09	88.06	1

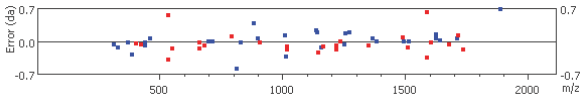
Disulfide bond



Reduced



#	b	b-H2O	b-NH3	b (2+)	Seq	y	y-H2O	y-NH3	y (2+)	#
1	100.08	82.07	83.05	50.54	V					18
2	260.11	242.10	243.08	130.55	C(+57.02)	1964.83	1946.82	1947.80	982.91	17
3	331.28	313.13	314.19	166.07	A	1804.80	1786.78	1787.77	902.90	16
4	388.45	370.15	371.18	194.58	G	1733.95	1715.75	1716.59	867.38	15
5	459.14	441.29	442.20	230.10	A	1676.82	1658.73	1659.71	838.87	14
6	556.26	538.24	539.23	278.63	P	1605.72	1588.04	1588.04	803.35	13
7	716.28	698.29	699.25	358.64	C(+57.02)	1508.79	1490.64	1491.52	754.82	12
8	829.41	811.36	812.93	415.19	L	1348.71	1330.61	1331.59	674.81	11
9	900.34	882.00	883.38	450.70	A	1235.52	1217.63	1218.68	618.27	10
10	1029.45	1011.30	1012.76	515.22	E	1164.61	1146.73	1147.47	582.75	9
11	1157.64	1139.25	1140.28	579.25	Q	1035.45	1017.63	1018.55	518.23	8
12	1271.35	1253.61	1254.34	636.28	N	907.43	889.38	890.37	454.20	7
13	1384.62	1366.62	1367.53	692.82	I	793.23	775.34	776.32	397.18	6
14	1513.66	1495.69	1496.65	757.34	E	680.37	662.30	663.40	340.63	5
15	1642.69	1624.55	1625.61	821.86	E	551.39	533.62	533.62	276.11	4
16	1729.75	1711.74	1712.65	865.38	S	422.25	404.23	405.15	211.59	3
17	1889.08	1871.77	1872.76	945.39	C(+57.02)	335.15	317.14	318.12	168.07	2
18					R	175.12	157.11	158.09	88.06	1



	Peptide	Plog10
Not reduced	**R.VC(-1.01)AGAPC(-1.01)LAEQNIEESC(+57.02)R.I**	**97.81**
Reduced	R.VC(+57.02)AGAPC(+57.02)LAEQNIEESC(+57.02)R.I	104.48